

PROTEIN TRANSLOCATION

Structure of the posttranslational Sec protein-translocation channel complex from yeast

Samuel Itskanov¹ and Eunyoung Park^{2*}

The Sec61 protein-conducting channel mediates transport of many proteins, such as secretory proteins, across the endoplasmic reticulum (ER) membrane during or after translation. Posttranslational transport is enabled by two additional membrane proteins associated with the channel, Sec63 and Sec62, but its mechanism is poorly understood. We determined a structure of the Sec complex (Sec61-Sec63-Sec71-Sec72) from *Saccharomyces cerevisiae* by cryo-electron microscopy (cryo-EM). The structure shows that Sec63 tightly associates with Sec61 through interactions in cytosolic, transmembrane, and ER-luminal domains, prying open Sec61's lateral gate and translocation pore and thus activating the channel for substrate engagement. Furthermore, Sec63 optimally positions binding sites for cytosolic and luminal chaperones in the complex to enable efficient polypeptide translocation. Our study provides mechanistic insights into eukaryotic posttranslational protein translocation.

The eukaryotic Sec61 or prokaryotic SecY complex forms a universally conserved protein-conducting channel that is essential for biogenesis of many proteins (1–3). The channel mediates transport of soluble (e.g., secretory) proteins across the eukaryotic endoplasmic reticulum (ER) membrane or the prokaryotic plasma membrane through its water-filled pore and integration of membrane proteins into the lipid phase through its lateral gate. The Sec61/SecY channel consists of an hourglass-shaped α subunit, which contains 10 transmembrane segments (TMs 1 to 10), and two small β and γ subunits, which are single-pass membrane proteins in eukaryotes (4). Often, translocation is coupled with translation (i.e., cotranslational translocation) by direct docking of a translating ribosome onto the channel. The channel also translocates many proteins in a posttranslational manner, the mechanisms of which differ between eukaryotes and prokaryotes. In eukaryotes, posttranslational translocation requires two essential membrane proteins, Sec63 and Sec62, which associate with the channel (5–8), and the ER-resident Hsp70 chaperone BiP, which grasps the substrate polypeptide in the ER lumen and prevents it from backsliding to the cytosol (9–12). In fungal species, the complex (hereafter referred to as the Sec complex) is further associated with the nonessential Sec71 and Sec72 subunits (10, 11, 13). The molecular architecture of the Sec complex and the functions of its subunits are poorly defined.

To gain insight into Sec-mediated protein translocation, we determined a structure of the

Saccharomyces cerevisiae Sec complex at 3.7-Å resolution by cryo-electron microscopy (cryo-EM) (Fig. 1 and figs. S1 and S2). Many side chains are clearly visible in the density map, enabling modeling of an accurate atomic structure (Fig. 1B and fig. S2C). The map also allowed us to improve the model for the eukaryotic Sec61 channel, which was previously built into maps at ~4- to 5-Å local resolutions (14, 15). However, Sec62 and the ER-luminal J domain of Sec63, which transiently interacts with BiP

(9–11, 16), were not sufficiently resolved for model building, likely because of their flexible motions (Fig. 1A). The structure reveals that Sec63 together with Sec71-Sec72 forms a large soluble domain, which sits on the cytosolic side of the Sec61 channel (Fig. 1). Sec63 consists of an N-terminal domain containing three TMs and a J domain between the second and third TMs and a C-terminal cytosolic domain (Fig. 2, A and B). The cytosolic domain contains two α helical domains (HD1 and HD2) and an immunoglobulin-like [fibronectin type-III (FN3)] domain, which are arranged similarly to the homologous region of the Brr2 RNA helicase (17) (fig. S3). Sec71-Sec72, the structure of which is similar to a recent crystal structure of *Chaetomium thermophilum* Sec71-Sec72 (18), clamps Sec63's cytosolic domain like tongs (fig. S4).

Sec63 makes extensive contacts with the channel through its transmembrane, cytosolic, and luminal domains, indicative of a major role in regulating the channel's function (Fig. 2, C to E). In the membrane region, the TMs of Sec63 are located at the back (opposite from the lateral gate) of the Sec61 channel, interacting with the TMs of Sec61 β and Sec61 γ as well as TM1 and TM5 of Sec61 α (Fig. 2C). Considering the extensive interactions between these elements, the TMs of Sec63 likely make a main contribution to the association between Sec61 and the rest of the Sec complex. In the cytosolic region, the FN3 domain of Sec63 interacts with the loop between TM6 and TM7 (L6/7) of Sec61 α through antigen-antibody-like binding. Like other FN3 domains, FN3 of Sec63 has a canonical β -sandwich fold composed of seven β strands (referred to as

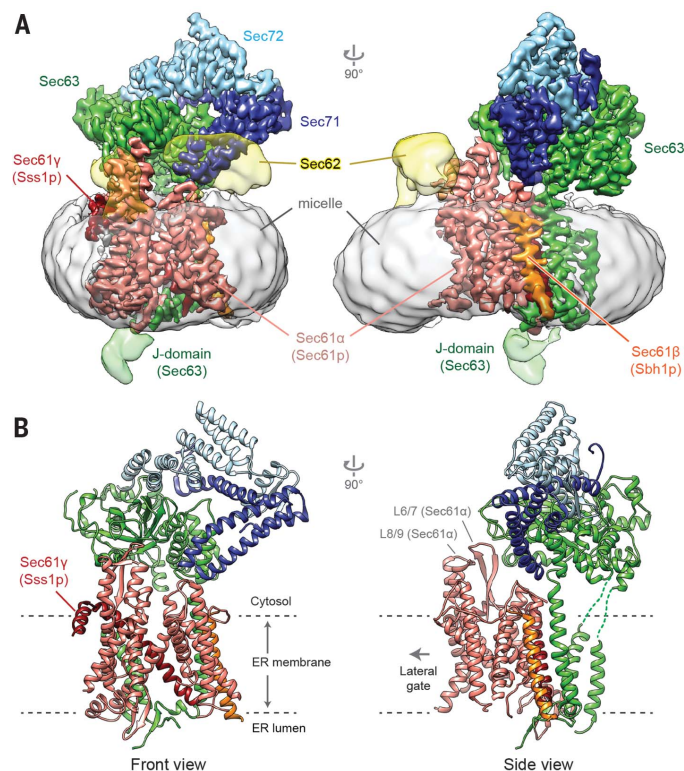


Fig. 1. Structure of the yeast Sec complex. (A) Cryo-EM density map and (B) atomic model of the yeast post-translational protein translocation complex. The front view is a view into the lateral gate.

¹Biophysics Graduate Program, University of California, Berkeley, Berkeley, CA 94720, USA. ²Department of Molecular and Cell Biology and California Institute for Quantitative Biosciences, University of California, Berkeley, Berkeley, CA 94720, USA.

*Corresponding author. Email: eunyoung_park@berkeley.edu

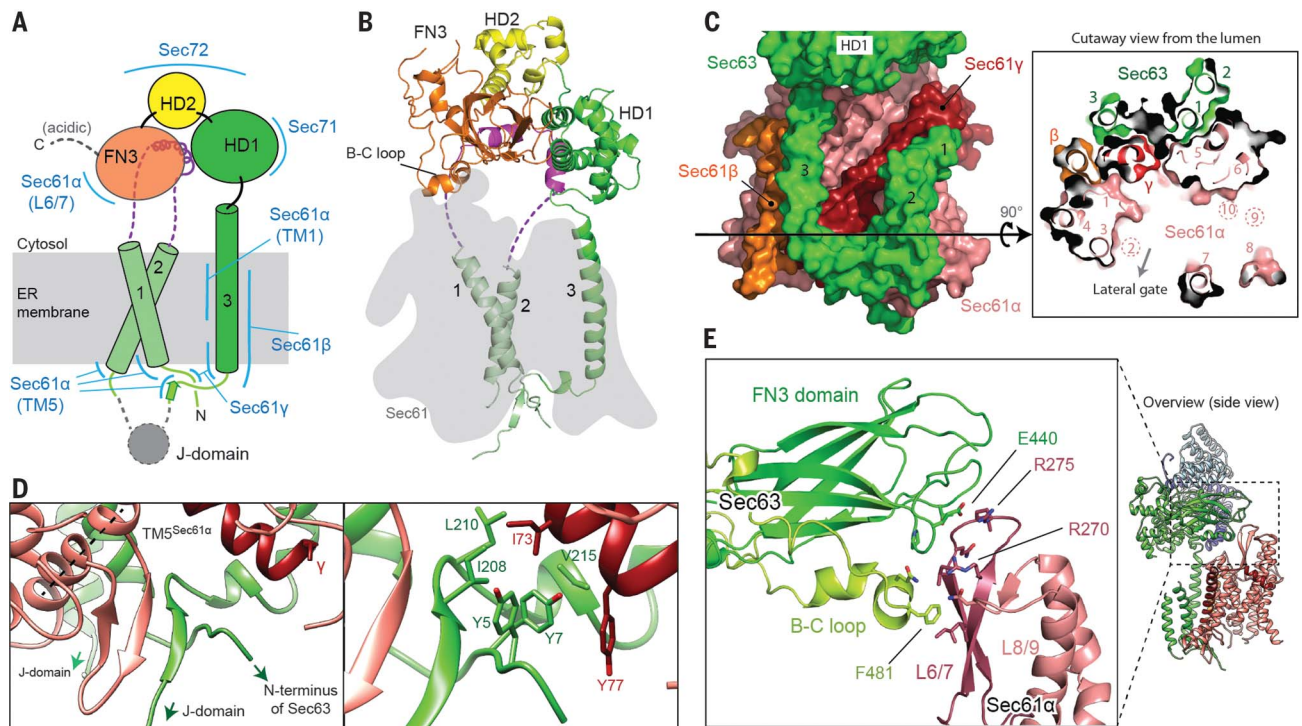
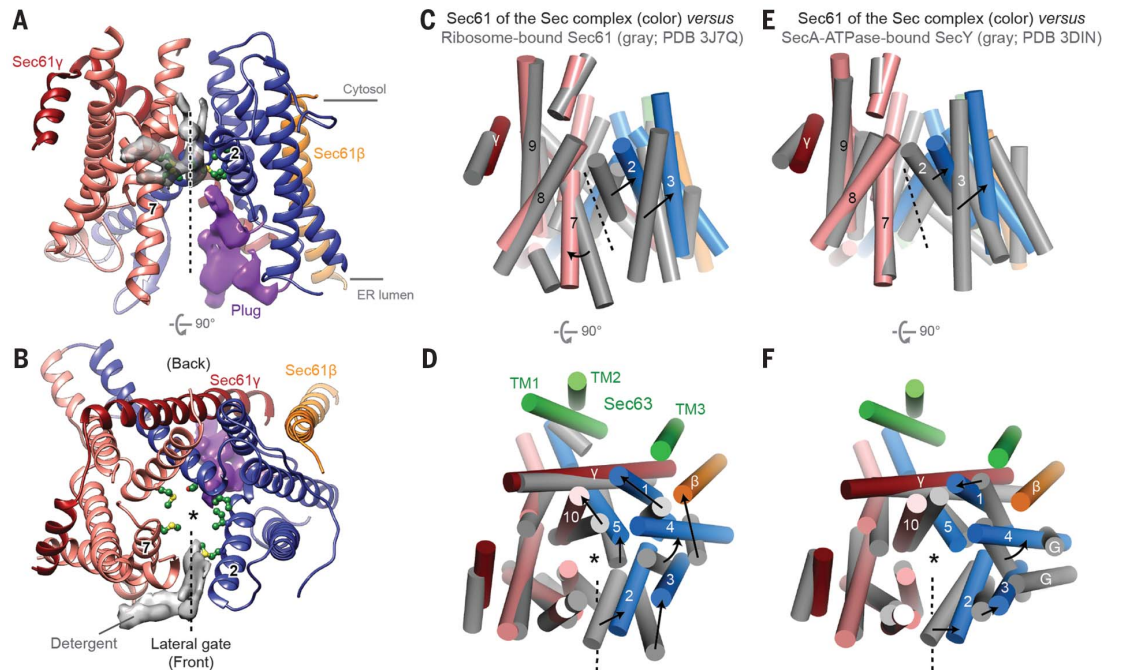


Fig. 2. Structure of Sec63 and its interactions with the channel.

(A) Schematic of Sec63 domains. Regions interacting with other parts of the complex are indicated by blue lines. Unmodeled regions are shown with dashed lines. (B) Structure of Sec63 (front view). The position of Sec61 is shaded in gray. (C) Interactions between TMs of Sec63 and Sec61. On the left is a view from the back; on the right is a cutaway view from the ER lumen. The black arrowed line represents the cross-sectional

plane. TMs 2, 9, and 10 of Sec61 α are located above the cross-sectional plane. (D) Interactions between Sec63 and Sec61 in the luminal side. On the left is a β sheet formed between Sec61 α (TM5 indicated by a dashed line) and the segment between Sec63 TM3 and the J domain. On the right is a magnified view with side chains shown as sticks. (E) Interactions between the FN3 domain and the cytosolic loop L6/7 of Sec61 α (also see Fig. 1B). L, Leu; I, Ile; V, Val; Y, Tyr; E, Glu; R, Arg; F, Phe.

Fig. 3. A fully opened Sec61 channel in the Sec complex. (A and B) Structure of the Sec61 channel. The N- and C-terminal halves of Sec61 α are in blue and salmon, respectively. The gray density feature is presumed detergent molecules. Pore-lining residues are shown as green balls and sticks. The density feature for the plug is in purple. Numbers "2" and "7" indicate TM2 and TM7, respectively. (C to F) Comparison of Sec61 of the Sec complex (colored) with Sec61 of the cotranslational ribosome-Sec61 complex [gray; (C) and (D)] or SecY of a bacterial post-translational SecA-SecY channel complex [gray; (E) and (F)]. The structures are aligned with respect to the C-terminal half of Sec61 α [(C) to (F)]. Shown are the front [(A), (C), and (E)] and cytosolic [(B), (D), and (F)] views. Numbers indicate corresponding TMs. Dashed lines represent the lateral gate. Asterisks indicate the translocation pore. For simplicity, L6/7 and L8/9 of Sec61 α are not shown. In (D) and (F), TMs of Sec63 are also shown (green). In (F), TMs of SecG are indicated by "G." Also see fig. S6 for comparisons to archaeal SecY and substrate-engaged channels. ATPase, adenosine triphosphatase; PDB, Protein Data Bank.



(A) and (B) Structure of the Sec61 channel. The N- and C-terminal halves of Sec61 α are in blue and salmon, respectively. The gray density feature is presumed detergent molecules. Pore-lining residues are shown as green balls and sticks. The density feature for the plug is in purple. Numbers "2" and "7" indicate TM2 and TM7, respectively. (C to F) Comparison of Sec61 of the Sec complex (colored) with Sec61 of the cotranslational ribosome-Sec61 complex [gray; (C) and (D)] or SecY of a bacterial post-translational SecA-SecY channel complex [gray; (E) and (F)]. The structures are aligned with respect to the C-terminal half of Sec61 α [(C) to (F)]. Shown are the front [(A), (C), and (E)] and cytosolic [(B), (D), and (F)] views. Numbers indicate corresponding TMs. Dashed lines represent the lateral gate. Asterisks indicate the translocation pore. For simplicity, L6/7 and L8/9 of Sec61 α are not shown. In (D) and (F), TMs of Sec63 are also shown (green). In (F), TMs of SecG are indicated by "G." Also see fig. S6 for comparisons to archaeal SecY and substrate-engaged channels. ATPase, adenosine triphosphatase; PDB, Protein Data Bank.

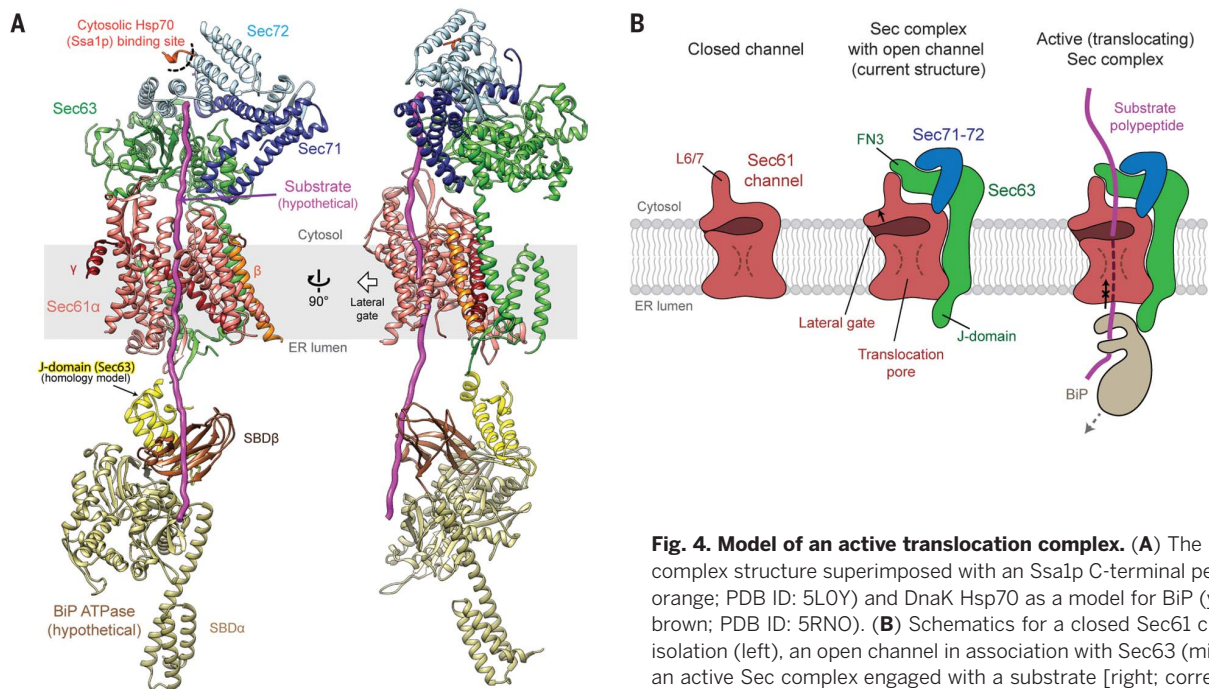


Fig. 4. Model of an active translocation complex. (A) The Sec complex structure superimposed with an Ssa1p C-terminal peptide (red orange; PDB ID: 5LOY) and DnaK Hsp70 as a model for BiP (yellow and brown; PDB ID: 5RNO). **(B)** Schematics for a closed Sec61 channel in isolation (left), an open channel in association with Sec63 (middle), and an active Sec complex engaged with a substrate [right; corresponding to the model in (A)]. For the full translocation cycle, see fig. S8.

A to G) but contains unusually long A-B, B-C, and D-E interstrand loops (fig. S3, B and C). With both A-B and B-C loops, FN3 creates a binding surface for L6/7, which uses a combination of surface complementarity and electrostatic and hydrophobic interactions (Fig. 2E and fig. S3D). Although sequence conservation is not obvious, metazoan Sec63s have similar extensions in the A-B and B-C loops. We expect analogous interactions between Sec63 and Sec61 in other eukaryotes. The interaction between FN3 and L6/7 is noteworthy because L6/7, together with L8/9, forms a docking site for the ribosome (14, 19, 20) (fig. S5A). Accordingly, superimposition of the Sec complex with a ribosome-bound Sec61 structure shows massive steric clashes between the ribosome and the cytosolic domains of Sec63 and Sec62 (fig. S5B), explaining why Sec61 in the Sec complex cannot bind to the ribosome (7, 11). In the ER luminal side, a segment preceding TM3 of Sec63 is directed into the luminal funnel of the Sec61 channel through the crevice present between TM5 of Sec61 α and the TM of Sec61 γ (Fig. 2D). This segment makes an antiparallel β sheet together with a β hairpin looping out in the middle of Sec61 α 's TM5. This β -augmentation is further buttressed by hydrophobic interactions with the N-terminal segment of Sec63. These features are highly conserved throughout eukaryotes and thus likely play an important role in optimal positioning of the J domain.

One pronounced feature of the Sec complex structure is a fully open channel (Fig. 3, A and B). The Sec61/SecY channel has a characteristic clamshell-like topology, in which its central pore can open toward the lipid phase through the lateral gate formed between TM2 and TM7.

Compared with previous Sec61/SecY structures (4, 14, 21–24), the channel in the Sec complex displays a substantially wider opening at its lateral gate, through which a signal sequence can readily pass as an α helix (Fig. 3 and fig. S6). This contrasts with structures of channels associated with the ribosome or the bacterial posttranslational translocation motor SecA (14, 21–24), in which the channel shows an only partially open lateral gate (Fig. 3, C to F), which was proposed to be further opened by interaction with the hydrophobic signal sequence during the initial substrate insertion. The opening is achieved by a largely rigid-body movement between the two halves (TMs 1 to 5 and 6 to 10) of Sec61 α and additional motions of the lateral gate helices. The fully open conformation appears to be a result of the extensive interactions with Sec63. For example, binding between FN3 and L6/7 perhaps pulls the C-terminal half of Sec61 α to open the lateral gate. However, further investigation will be necessary to understand the precise mechanism and the dynamics of channel gating in the native membrane environment. At the open lateral gate slit, there is a weak density feature, which likely represents bound detergent molecules (Fig. 3, A and B). In the native membrane, lipid molecules may occupy this site and facilitate initial binding of signal sequences.

Our channel structure likely also represents a fully open state of the translocation pore (Fig. 3B and fig. S7). The radius of the pore constriction is ~ 3 Å, large enough to pass an extended polypeptide chain. The opening would also permit passage of small hydrated ions and polar molecules in the absence of a translocating polypeptide (25, 26), although the relatively positive electro-

static potential around the pore may disfavor permeation of positively charged species (fig. S7C). Yeast Sec61 has a relatively less hydrophobic pore constriction compared with nonfungal Sec61 and prokaryotic SecY (fig. S7D). In prokaryotes, reduction of hydrophobicity in the pore constriction has been shown to lead to membrane potential dissipation (26), and similarly, in higher eukaryotes it might cause calcium leakage from the ER. However, yeast may tolerate ion leakage because calcium is stored primarily in the vacuole. In resting or primed channels, the pore is closed or narrow (< 2 Å in radius) and further blocked by a small α -helical plug in the luminal funnel (4, 14, 21). By contrast, in our structure, the plug seems flexible and displaced from the pore (Fig. 3, A and B).

The spatial arrangement of Sec63 and Sec71–Sec72 with respect to the Sec61 channel suggests how these components play roles in accepting a polypeptide substrate from a cytosolic chaperone and handing it over to the channel and subsequently to BiP. Studies of *C. thermophilum* Sec72 have suggested that Sec72 provides a docking site for the cytosolic Hsp70 chaperone Ssa1p (18), which prevents substrates from premature folding or aggregation before translocation (6). Superimposition of the cocrystal structure of Sec72 and an Ssa1p C-terminal tail shows that the Ssa1p-binding site is ~ 60 Å above the channel's pore (Fig. 4A). While the cytosolic domain of Sec63–71–72 sits on top of Sec61, its position is tilted such that the polypeptide can insert straight down to the pore. Similarly, Sec62 is also positioned off the translocation path (Fig. 1A). Thus, upon release from Ssa1p, a substrate would efficiently engage with the pore without obstruction. The

structure also allows us to propose how BiP Hsp70 may catch the substrate in the ER lumen. Despite the low resolution of the J domain (Fig. 1A), we could dock a homology model into the EM density map based on the shape of the feature and the orientations of the flanking segments (Fig. 4A). We then superimposed a recent crystal structure of a bacterial J domain–Hsp70 complex (27) to our EM structure (Fig. 4A). This modeling exercise showed that a peptide-binding cleft of the Hsp70 [called substrate-binding domain β (SBD β)] would be placed directly below the translocation pore. Thus, the J domain seems optimally positioned to allow BiP to grasp the substrate polypeptide as it emerges from the channel.

Our structure offers a model for how Sec63 enables posttranslational translocation (Fig. 4B and fig. S8) and provides a more complete picture of how the Sec61/SecY channel works together with different binding partners (i.e., ribosomes, Sec63, or SecA) to enable transport of a range of substrates. Association of Sec63 seems to induce full opening of the channel, a conformation in which the channel can readily accept a substrate polypeptide. Such a conformation, compared with a partially open channel seen with the other modes, is likely advantageous for many posttranslational-specific substrates, which tend to have a less hydrophobic signal sequence (28–30).

REFERENCES AND NOTES

1. E. Park, T. A. Rapoport, *Annu. Rev. Biophys.* **41**, 21–40 (2012).
2. R. M. Voorhees, R. S. Hegde, *Curr. Opin. Cell Biol.* **41**, 91–99 (2016).
3. E. C. Mandon, S. F. Trueman, R. Gilmore, *Cold Spring Harb. Perspect. Biol.* **5**, a013342 (2013).
4. B. Van den Berg *et al.*, *Nature* **427**, 36–44 (2004).
5. J. A. Rothblatt, R. J. Deshaies, S. L. Sanders, G. Daum, R. Schekman, *J. Cell Biol.* **109**, 2641–2652 (1989).
6. R. J. Deshaies, S. L. Sanders, D. A. Feldheim, R. Schekman, *Nature* **349**, 806–808 (1991).
7. H. A. Meyer *et al.*, *J. Biol. Chem.* **275**, 14550–14557 (2000).
8. J. Tyedmers *et al.*, *Proc. Natl. Acad. Sci. U.S.A.* **97**, 7214–7219 (2000).
9. D. Feldheim, J. Rothblatt, R. Schekman, *Mol. Cell. Biol.* **12**, 3288–3296 (1992).
10. J. L. Brodsky, R. Schekman, *J. Cell Biol.* **123**, 1355–1363 (1993).
11. S. Panzner, L. Dreier, E. Hartmann, S. Kostka, T. A. Rapoport, *Cell* **81**, 561–570 (1995).
12. K. E. Matlack, B. Misselwitz, K. Plath, T. A. Rapoport, *Cell* **97**, 553–564 (1999).
13. N. Green, H. Fang, P. Walter, *J. Cell Biol.* **116**, 597–604 (1992).
14. R. M. Voorhees, I. S. Fernández, S. H. Scheres, R. S. Hegde, *Cell* **157**, 1632–1643 (2014).
15. K. Braunger *et al.*, *Science* **360**, 215–219 (2018).
16. K. E. Matlack, K. Plath, B. Misselwitz, T. A. Rapoport, *Science* **277**, 938–941 (1997).
17. T. H. Nguyen *et al.*, *Structure* **21**, 910–919 (2013).
18. A. Tripathi, E. C. Mandon, R. Gilmore, T. A. Rapoport, *J. Biol. Chem.* **292**, 8007–8018 (2017).
19. Z. Cheng, Y. Jiang, E. C. Mandon, R. Gilmore, *J. Cell Biol.* **168**, 67–77 (2005).
20. T. Becker *et al.*, *Science* **326**, 1369–1373 (2009).
21. J. Zimmer, Y. Nam, T. A. Rapoport, *Nature* **455**, 936–943 (2008).
22. P. F. Egea, R. M. Stroud, *Proc. Natl. Acad. Sci. U.S.A.* **107**, 17182–17187 (2010).
23. R. M. Voorhees, R. S. Hegde, *Science* **351**, 88–91 (2016).
24. L. Li *et al.*, *Nature* **531**, 395–399 (2016).
25. D. Heritage, W. F. Wonderlin, *J. Biol. Chem.* **276**, 22655–22662 (2001).
26. E. Park, T. A. Rapoport, *Nature* **473**, 239–242 (2011).
27. R. Kityk, J. Kopp, M. P. Mayer, *Mol. Cell* **69**, 227–237.e4 (2018).
28. D. T. Ng, J. D. Brown, P. Walter, *J. Cell Biol.* **134**, 269–278 (1996).
29. M. A. Smith, W. M. Clemons Jr., C. J. DeMars, A. M. Flower, *J. Bacteriol.* **187**, 6454–6465 (2005).
30. S. F. Trueman, E. C. Mandon, R. Gilmore, *J. Cell Biol.* **199**, 907–918 (2012).

ACKNOWLEDGMENTS

We thank D. Toso for help with electron microscope operation and J. Hurley, S. Brohawn, and K. Tucker for critical reading of the manuscript. **Funding:** This work was funded by UC Berkeley (E.P.) and an NIH training grant (T32GM008295; S.I.). **Author contributions:** S.I. and E.P. performed experiments, interpreted results, and wrote the manuscript; E.P. conceived and supervised the project. **Competing interests:** None declared. **Data and materials availability:** The cryo-EM density maps and atomic model have been deposited in EM Data Bank (accession code: EMD-0336) and Protein Data Bank (accession code: 6N3Q), respectively.

SUPPLEMENTARY MATERIALS

www.sciencemag.org/content/363/6422/84/suppl/DC1
Materials and Methods
Figs. S1 to S8
Table S1
References (31–40)

9 October 2018; accepted 21 November 2018
Published online 13 December 2018
10.1126/science.aav6740

Structure of the posttranslational Sec protein-translocation channel complex from yeast

Samuel Itskanov and Eunyong Park

Science **363** (6422), 84-87.

DOI: 10.1126/science.aav6740 originally published online December 13, 2018

Posttranslational translocon architecture

About a third of proteins are transported into endoplasmic reticulum by the universally conserved Sec61 protein-conducting channel. Itskanov and Park determined a cryo-electron microscopy structure of the Sec complex from yeast, which mediates posttranslational translocation of many secretory proteins across the endoplasmic reticulum membrane. The study reveals how Sec63 activates the Sec61 channel for substrate polypeptide insertion. The structure also explains the mutually exclusive binding of Sec63 and the ribosome to the channel.

Science, this issue p. 84

ARTICLE TOOLS

<http://science.sciencemag.org/content/363/6422/84>

SUPPLEMENTARY MATERIALS

<http://science.sciencemag.org/content/suppl/2018/12/12/science.aav6740.DC1>

REFERENCES

This article cites 40 articles, 19 of which you can access for free
<http://science.sciencemag.org/content/363/6422/84#BIBL>

PERMISSIONS

<http://www.sciencemag.org/help/reprints-and-permissions>

Use of this article is subject to the [Terms of Service](#)

Science (print ISSN 0036-8075; online ISSN 1095-9203) is published by the American Association for the Advancement of Science, 1200 New York Avenue NW, Washington, DC 20005. The title *Science* is a registered trademark of AAAS.

Copyright © 2019 The Authors, some rights reserved; exclusive licensee American Association for the Advancement of Science. No claim to original U.S. Government Works